Tree Physiology 26, 275–284

Transpiration-induced axial and radial tension gradients in trunks of Douglas-fir trees

J.-C. DOMEC,[1,2] F. C. MEINZER,[3] B. L. GARTNER[1] and D. WOODRUFF[3,4]

[1] *Department of Wood Science and Engineering, Oregon State University, Corvallis, OR 97331, USA*

[2] *Corresponding author (jc.domec@oregonstate.edu)*

[3] *USDA Forest Service, Forestry Sciences Laboratory, 3200 SW Jefferson Way, Corvallis, OR 97331, USA*

[4] *Department of Forest Science, Oregon State University, Corvallis, OR 97331, USA*

Received January 11, 2005; accepted June 11, 2005; published online December 15, 2005

Summary We determined the axial and radial xylem tension gradients in trunks of young Douglas-fir (*Pseudotsuga menziesii* (Mirb.) Franco) trees. Axial specific conductivity ($k_{s\text{-}a}$) and sap flux density (J_s) were measured at four consecutive depths within the sapwood at a stem height of 1 m. By definition, at a given position in the bole, J_s is a function not only of $k_{s\text{-}a}$ but also of the driving force for water movement. The J_s:$k_{s\text{-}a}$ ratio was therefore used to estimate axial tension gradients and the radial gradients at a stem height of 1 m were calculated from the differences in axial tension gradients at each depth. Tracheid lumen diameter and tracheid length were used to predict differences in $k_{s\text{-}a}$ and its divergence from the theoretical $k_{s\text{-}a}$ determined by the Hagen Poisseuille equation. The ratio of $k_{s\text{-}a}$ (determined in the laboratory) to J_s (measured in the field) varied with depth in the sapwood, resulting in non-uniform axial and radial tension gradients from inner to outer sapwood. Transpiration-induced axial tension gradients were in the range of 0.006–0.01 MPa m^{-1} excluding the gravitational tension gradient. At a stem height of 1 m, radial tension gradients were in the range of 0.15–0.25 MPa m^{-1} and were lower in the middle sapwood than in the inner or outer sapwood. Axial tension gradients were 44–50% higher in the outer sapwood than in the inner sapwood. At a stem height of 1 m, radial J_s, calculated on the basis of radial tension gradients and measured radial specific conductivity ($k_{s\text{-}r}$), was about two orders of magnitude smaller than axial J_s. Our findings indicate that large radial tension gradients occur in the sapwood and clarify the role played by xylem $k_{s\text{-}a}$ and $k_{s\text{-}r}$ in determining in situ partitioning of J_s in the axial and radial directions.

Keywords: sap flux density, specific conductivity, xylem anatomy, xylem embolism.

Introduction

In a broad sense, the biophysical process by which xylem sap is transported to the tops of trees appears to be well understood. According to the Cohesion–Tension (C–T) theory, the driving force for water movement is generated by transpirational water loss, which transmits tension or negative pressure through continuous water columns extending from the evaporative surfaces in the leaves to the roots (Dixon 1914). When transpiration is absent, gravitational forces should result in a minimum standing xylem tension gradient of 0.01 MPa m^{-1} (Scholander et al. 1965). When transpiration occurs, frictional resistances make the axial tension gradient considerably steeper (Hellkvist et al. 1974, Domec and Gartner 2002, Woodruff et al. 2004). The C–T theory is compatible with Ohm's law electrical analogues often applied to predict and account for water movement along the soil-plant-atmosphere continuum. In transpiring trees, models based on Ohm's law yield estimates of axial tension gradients ranging from as low as 0.005 MPa m^{-1} in trunks to as high as 1 MPa m^{-1} in small branches (Tyree 1988, Tyree et al. 1991).

Sapwood axial specific hydraulic conductivity of the xylem ($k_{s\text{-}a}$; kg m^{-1} MPa^{-1} s^{-1}) can be determined by measuring the rate of flow through a wood specimen of known length and cross-sectional area while a known pressure gradient is applied. Sap flux density (J_s; kg m^{-2} s^{-1}) in intact trees can be determined empirically by techniques that involve localized application of heat as a tracer (Cohen et al. 1981, Granier 1985). Given that the flow of water through a stem can be described by formulating Darcy's law as $J_s = k_{s\text{-}a}(\partial P/\partial x)$, where $\partial P/\partial x$ (MPa m^{-1}) is the hydrostatic pressure gradient, paired measurements of overall $k_{s\text{-}a}$ and J_s provide a means of estimating transpiration-induced hydrostatic pressure gradients in intact stems. The ability to characterize radial variation in J_s and $k_{s\text{-}a}$ across the sapwood would permit assessment of radial variation in axial tension gradients as well as radial tension gradients between the innermost and outermost conducting xylem. Recently, techniques have been developed that allow measurement of detailed radial profiles of $k_{s\text{-}a}$ (Spicer and Gartner 1998) and J_s (Cohen et al. 1981, James et al. 2002) in tree trunks. However, we know of no studies that have employed these methods to estimate axial and radial tension gradients in the xylem of intact, transpiring trees.

In several species, J_s is reported to be maximal at one to several cm inward from the cambium rather than adjacent to the

cambium (Phillips et al. 1996, Nadezhdina et al. 2002, James et al. 2003). However, it is unclear whether this pattern is the result of a larger axial tension gradient or greater $k_{s\text{-}a}$ at these depths (Mark and Crews 1973, Spicer and Gartner 2001, Gartner and Meinzer 2005). In a tree, the xylem of leaves produced during a given year is connected directly to the stem xylem formed during the same year. Assuming that leaves are supplied with water primarily through xylem produced in the same year (Tison 1903), the axial tension gradient should be greatest in the outermost growth rings, resulting in a radial gradient of decreasing tension from the outer- to the innermost rings. Therefore, the highest J_s in the trunk is likely to occur in the growth rings that are more directly connected to existing cohorts of transpiring leaves.

Although general patterns of axial water transport in tree trunks are widely reported, little quantitative information is available about the radial flow of water across growth rings. In the absence of reliable techniques to detect radial water movement, determinations of sap flow typically ignore radial deviation of sap from the axial path. In conifers, most inter-tracheid pits are on radial rather than tangential cell walls, facilitating water movement within a growth ring but not between growth rings (Panshin and de Zeeuw 1980). In addition, the decrease in tracheid size from outer to inner sapwood is correlated with lower pit density and thicker pit chambers (Panshin and de Zeeuw 1980), which increases the effect of pit resistance on water transport in the radial direction (Calkin et al. 1986). Radial specific conductivity ($k_{s\text{-}r}$) should therefore be higher in the outer sapwood than in the inner sapwood. Measurements of $k_{s\text{-}r}$ combined with the radial tension gradient would allow estimation of the relative importance of radial sap flow from inner to outer rings.

The aim of this study was to estimate in situ axial and radial tension gradients in trunks of Douglas-fir trees based on radial profiles of J_s and $k_{s\text{-}a}$. Heat dissipation probes were used to determine daily time courses of J_s at four radial depths in the trunks of 24-year-old trees. The trees were then felled to obtain samples of sapwood for determination of $k_{s\text{-}a}$ at the locations where J_s was measured. We determined $k_{s\text{-}r}$ on wood cores extracted near the locations where J_s and $k_{s\text{-}a}$ were measured. In addition to providing estimates of in situ axial and radial tension gradients, this procedure allowed us to estimate the relative magnitude of radial J_s compared with axial J_s.

Materials and methods

Field site and plant material

The study was carried out from September to November 2002 in a Douglas-fir (*Pseudotsuga menziesii* Mirb. Franco) stand planted in 1978 on a clear-cut located within the Wind River Experimental Forest near the Wind River Canopy Crane Research Facility in southern Washington (45°49′ N, 121°57′ W) at an elevation of 560 m. The 24-year-old trees were about 16 m tall and 0.2 m in diameter at a height of 1.3 m. Stand density was about 1300 trees ha^{-1}. Although mean annual precipitation is about 2500 mm, < 120 mm precipitation falls between June and September. Photosynthetic photon flux (PPF) and vapor pressure deficit (VPD) during the study were obtained from an automated weather station installed 4 m above the canopy.

Sap flow density

Four healthy, uniform trees were selected for installation of sap flow sensors in September. Variable length heat dissipation sap flow probes with a heated and a reference sensor of 10 mm at the probe tip (James et al. 2002) were used to determine J_s at radial depths of 1, 2, 3 and 4 cm at a stem height of 1.3 m. Sapwood depths and the boundary between heartwood and sapwood were determined visually from cores. The trees had 4.8 cm of sapwood, which represented 12 rings, with a 0.7 cm transition zone (two rings) between sapwood and heartwood. The outermost radial depth (1 cm) represented rings 1 and 2, and the deepest radial depth (4 cm) comprised rings 9 to 12. The pairs of sensors were installed at a height of 1.3 m on the north side of the trunk at four successive depths in a spiral around the bole, 10 cm apart both vertically and circumferentially. The probes were protected from sunlight and rainfall by reflective insulation. The signal from the sap flow probes was scanned every minute and 10-min means were recorded by a data logger (CR 10X; Campbell Scientific, Logan, UT) equipped with a 32-channel multiplexer (AM416; Campbell Scientific). Temperature difference between the two sensors (ΔT) was converted to J_s (g m^{-2} s^{-1}) based on the empirical calibration of Granier (1985), recently revalidated by Clearwater et al. (1999) and Ford et al. (2004):

$$J_s = 119k^{1.231} \quad (1)$$

where $k = (\Delta T_m - \Delta T)/\Delta T$ and ΔT_m is the temperature difference when sap flux is assumed to be zero.

Axial specific conductivity and field embolism

The four trees fitted with sap flow sensors were harvested at the end of November 2002. Disks about 25 cm thick, encompassing the sap flow sensor locations, were cut and immediately transported to the laboratory in wet polyethylene bags with both ends of each disk in contact with wet paper towels to limit evaporation from the xylem. The disks were stored at 3 °C on the day of harvest until blocks were prepared for measurement of $k_{s\text{-}a}$. Thinner second disks were also cut for measuring sapwood and heartwood areas (see below). From each of the 25-cm disks, replicate pairs of 90–110-mm-long blocks were taken near to the sensor locations at radial depths centered on 1, 2, 3 and 4 cm, for a total of eight blocks. Additionally, two extra blocks were taken at the outer edge of the sapwood, centered on 0.5 cm, where no sap flow sensors were present. The disks were split along the grain first with a maul and wedge and then with a chisel. The samples were then stored at 3 °C in wet paper towels until the next day when $k_{s\text{-}a}$ was measured as (Heine 1971):

$$k_{s-a} = \frac{VL}{tA\Delta P} \quad (2)$$

where V is the volume of water that went through the sample (converted to mass in kg), L is sample length (m), t is time (s), A is cross-sectional area (m^2) of the sample and ΔP is the pressure difference (MPa) between the sample ends. The entire cross-sectional area of each sample (92–96 mm^2) was assumed to be functional sapwood and was calculated from the mean of the cross-sectional areas of the two ends.

The conductivity apparatus (Spicer and Gartner 1998) consisted of a membrane-lined pressure sleeve attached to tubing filled with filtered (0.22 μm) water adjusted with HCl to pH 2 to prevent microbial growth. The samples were perfused at a hydraulic pressure head of 6 kPa, which was low enough to avoid refilling of embolized tracheids. The rate of efflux was measured in a 1-ml graduated pipette. When the flow was steady, the time required for the meniscus to cross 10 consecutive graduation marks (1 ml) was recorded. Native embolism was determined by comparing the initial (or native) axial specific conductivity ($k_{s-a(i)}$) of trunk segments to the maximum axial specific conductivity ($k_{s-a(max)}$) after removal of air emboli by soaking the samples under vacuum for 48 h. Percentage loss of conductivity (PLC) was computed as PLC = $100(1 - (k_{s-a(i)}/k_{s-a(max)}))$. Following each final conductivity measurement, samples were perfused with filtered (0.22 μm) safranin-O (0.2% aqueous solution) under a 15 kPa pressure head for 20 min while still enclosed in the pressure sleeve apparatus. The samples consistently stained completely, giving no evidence of residual embolism.

All conductivity calculations were corrected to 20 °C or to in situ stem temperature to account for changes in fluid dynamic viscosity. Stem temperature was estimated from air temperature measured at breast height assuming that air temperature oscillates sinusoidally with time (t) and has the form $T_{(t)} = T_a + \alpha\sin(2\pi t/24)$, where T_a is mean daily air temperature and α is amplitude (Monteith and Unsworth 1990). Harmonic change in stem temperature was then fitted by $T_{S(t)} = T_a + \alpha exp\phi\sin(2\pi t/24 - \phi)$, where ϕ is the phase lag of the response of stem temperature to air temperature and is given by $z/(24\kappa/\pi)^{1/2}$, where z is sapwood depth and κ is thermal diffusivity of the trunk (taken as 14.6×10^{-8} m^2 s^{-1}; Herrington 1969). The amplitude in the outermost and innermost sapwood was calculated to be 79 and 52% of the air amplitude, respectively. For a measured bark thickness of 1.5 cm, the phase lag response was 1 h 05 min in the outer sapwood and 2 h 15 min in the inner sapwood, which are in the same order as measured values for conifers (Herrington 1969).

Radial specific conductivity

Radial specific conductivity was measured by the high-pressure flow meter (HPFM) method (Tyree et al. 1993, Yang and Tyree 1994) on 12-mm-diameter sapwood cores taken at breast height. The sapwood cores were divided into outer (0.5–2.5 cm) and inner sections (2.5–4.5 cm). For k_{s-r}, the outer section represented sapwood rings 1 to 6 and the inner section represented sapwood rings 7 to 12. The flow meter consisted of a water tank that was pressurized with compressed air. Water flow rate through the core was computed from the measured pressure drop across a capillary tube of known resistance interposed between the tank and the sample. The HPFM was connected to the cores and perfused for 10 to 20 min at a pressure of 0.2 MPa with filtered (0.22 μm) water. The HPFM was calibrated by directing flow of water across a length of capillary tube via water-filled tubing to a container of water on a scale.

Xylem anatomical analyses

Earlywood tracheid lengths and earlywood lumen diameters were measured in each sample used to determine conductivity. An image analysis system consisting of a compound microscope, video camera, computer and NIH Image Version 1.60 (Rasband 1996) was used to analyze both tracheid macerations and transverse sections.

Samples for evaluating earlywood tracheid length were prepared by removing matchstick-sized wedges from the earlywood portion of each sample growth ring and macerating them in a solution of 20% nitric acid and 0.5% sodium chlorite (Spearing and Isenberg 1947). The macerations were washed, stained with safranin-O, mounted and viewed at 4× magnification with a compound microscope. Lengths of 80 randomly-selected tracheids per sample were measured.

Tracheid earlywood lumen diameter was determined on transverse sections (30 μm thick) of the proximal end of each sample obtained with a sliding microtome. Sections were stained in a 1% solution of safranin-O following a dehydration series, mounted and viewed at 40× magnification with a compound microscope. Inside diameters were calculated by measuring the lengths of lines drawn across the lumen. For each growth ring, six radial files of tracheids were randomly selected and the first 15 tracheids in each file produced outward from the growth ring boundary were measured in the radial direction for diameter. About 90 earlywood tracheids were measured per sample for each growth ring. Following the diameter measurements, earlywood tracheid density was calculated by dividing the total number of earlywood tracheids present in each growth ring by the earlywood area of the growth ring. Additionally, earlywood proportion was determined on the transverse sections by means of a one line scan through each sample. An average earlywood proportion for each sample was calculated as the mean of the average earlywood proportion of all the growth rings analyzed for that sample.

Because the latewood tracheid diameters were small, theoretical k_{s-a} of the xylem earlywood patch weighted by the proportion of earlywood tracheids was assumed to represent the theoretical k_{s-a} of the whole sample and was calculated according to the equation for capillaries (Calkin et al. 1986):

$$k_{s-a\ theoretical} = \frac{N\pi\rho\sum_{i=1}^{n} D_i^4}{128\eta n} \times W_e \quad (3)$$

where ρ is density of water (kg m^{-3}), N is tracheid density (m^{-2}), η is dynamic viscosity of water (MPa s), D is diameter of the ith tracheid summed over the number of tracheids, n, and W_e is proportion of earlywood.

Radial tension gradients

Radial tension gradients were calculated by first obtaining the differences in axial tension gradients (MPa m^{-1}) between adjacent depths and then dividing by the radial distances between them (0.01 m). If the axial tension gradient varies with depth in xylem, then a radial tension gradient would exist with units of MPa m^{-2} (i.e., MPa m_{axial}^{-1} m_{radial}^{-1}), which reflect the linear increase in radial tension gradient with height as a result of the increasing difference in the axial tension gradient between adjacent depths with height. Therefore, the actual radial tension gradients in the trunk expressed in units of MPa m_{radial}^{-1} depend on stem height. To be able to use the units of MPa m^{-1}, the radial tension gradients reported here are at a stem height of 1 m, close to where J_s and $k_{s\text{-}a}$ were measured. At this location, we assumed that the axial xylem tensions, rather than the axial gradients, were known at each radial depth. To correctly calculate the difference in axial tension gradient between adjacent depths we had to assume that water tensions in the inner and the outer sapwood returned to equilibrium at night. However, the water tension at the base of the trunk did not have to be zero for the radial tension gradients to be calculated, because by taking the differences in axial tensions at a given height, both the base values and the gravitational component canceled out. Concurrent soil and predawn leaf water potential measurements during the period studied indicated that the trees equilibrated with the soil, suggesting that nocturnal stomatal opening and transpiration did not occur and that, at a given stem height, different regions within the xylem were in equilibrium (Donovan et al. 2003). In addition, the ΔT_m between sap flow probes reached its maximum before 0300 h, consistent with the absence of water movement near the base of the tree.

Statistical analysis

Relationships between the hydraulic parameters and anatomical characteristics were fit by least squares methods. Effects of depth on hydraulic parameters were evaluated by analysis of variance (ANOVA), with tree as a blocking factor. The significance of the difference in hydraulic parameters between outer and inner sapwood was determined by paired t tests. All statistical procedures were conducted with Statistical Analysis Systems software (1999; SAS, Cary, NC).

Results

The diurnal course of J_s reflected diurnal changes in photosynthetically active radiation (PAR) with a sharp increase after sunrise, reaching a peak by 1100 h in the outer sapwood and decreasing in the late afternoon (Figure 1). On a sunny day (Day 266), J_s reached its peak and started to decline before VPD attained its maximum value. For both Day 266 and a cloudy fall day (Day 302) the increase in flow rate in the inner sapwood lagged that in the outer sapwood by ~60 minutes. The magnitude of J_s varied according to the depth of the sensors, and decreased from the outermost to the innermost sapwood.

Radial variation in J_s (Figure 2A) was associated with radial variation in $k_{s\text{-}a}$ (Figure 2B). Maximum values of $k_{s\text{-}a}$ were observed at depths of 0.5–2 cm in the outer sapwood and declined significantly toward the heartwood ($P < 0.02$). Native $k_{s\text{-}a}$ exhibited a similar radial profile, but was consistently 12–18% lower than maximum $k_{s\text{-}a}$ ($P < 0.03$), except at the outermost and innermost depths ($P > 0.4$). Inner sapwood had lower axial tension gradients than outer sapwood ($P = 0.03$, Figures 2C and 3). The transpiration-induced axial tension gradient decreased from 0.009 MPa m^{-1} in the outer sapwood

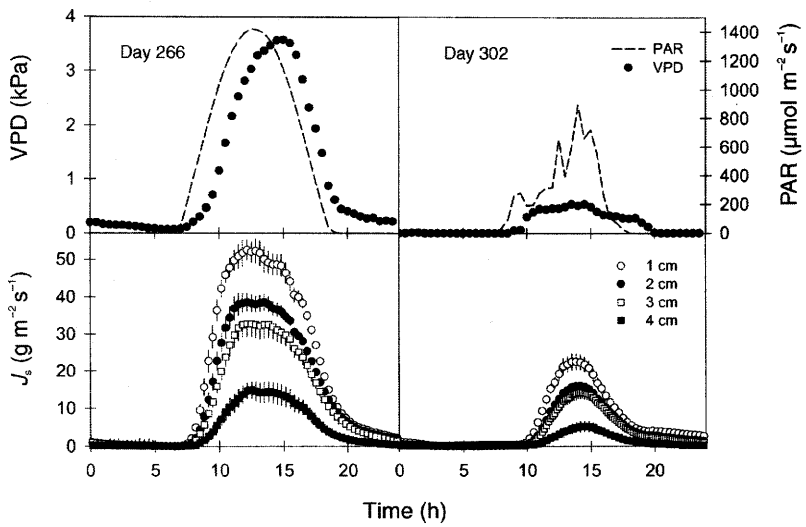

Figure 1. Diurnal courses of vapor pressure deficit (VPD), photosynthetically active radiation (PAR) and sap flux density (J_s) at four sapwood depths during a sunny summer day (Day 266) and a cloudy fall day (Day 302). Vertical bars represent standard errors.

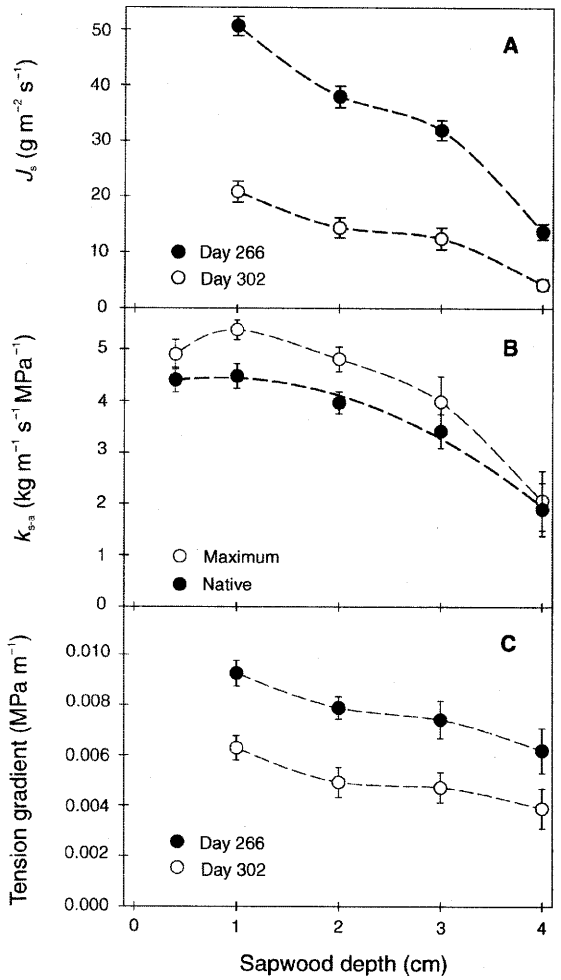

Figure 2: (A) Midday sap flux density (J_s) during a sunny summer day (Day 266) and a cloudy fall day (Day 302); (B) native and maximum (full saturation) axial specific conductivity (k_{s-a}); and (C) axial tension gradient in relation to radial sapwood depth. Vertical bars represent standard errors.

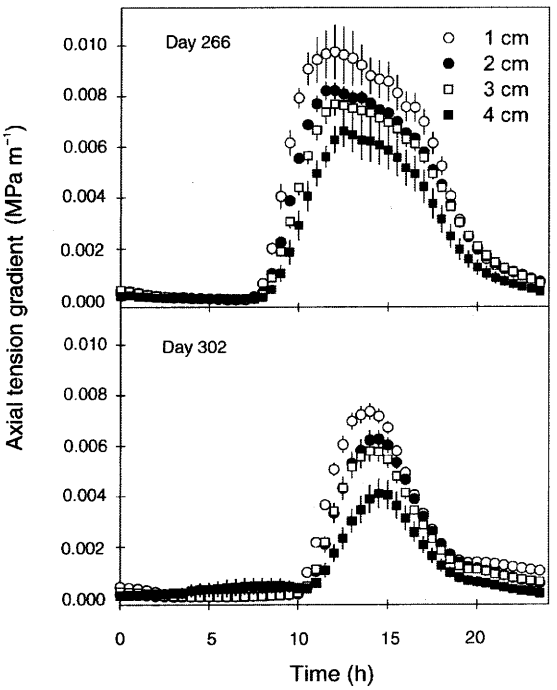

Figure 3. Diurnal courses of the axial xylem tension gradient at different sapwood depths during a sunny summer day (Day 266) and a cloudy fall day (Day 302). Vertical bars represent standard errors.

to 0.006 MPa m^{-1} in the inner sapwood during a sunny day, and from 0.006 MPa m^{-1} to 0.004 MPa m^{-1} during an overcast day (Figure 2C). The maximum axial tension gradient in the outer sapwood was close to 0.01 MPa m^{-1} during a sunny day and up to 0.007 MPa m^{-1} during an overcast day (Figure 3). For both days the increase in tension gradient in the inner sapwood lagged that in the outer sapwood by ~60 minutes. Maximum trunk temperature was calculated to be 3 and 7 °C lower than air temperature in the outer and inner sapwood, respectively (data not shown). Corrections of k_{s-a} for decreasing viscosities (lower temperature) from outer to inner sapwood did not result in significant changes in tension gradient.

At full saturation, k_{s-r} was about 2000 times lower than axial k_{s-a} (Table 1). Consistent with trends in k_{s-a}, outer sapwood had a higher k_{s-r} than inner sapwood, although the difference was not significant (Table 1). Radial tension gradients estimated from the difference in axial tension gradients between adjacent depths were lower in the middle sapwood than in the inner or outer sapwood ($P < 0.01$; Figure 4). At a stem height of 1 m, the maximum radial tension gradient in the outer sapwood was close to 0.25 MPa m^{-1} during a sunny day and up to 0.15 MPa m^{-1} during an overcast day. Assuming a constant rate of change in axial tension gradients with height, at a stem height of 10 m the radial tension would be greater than 2.0 MPa m^{-1}. Based on k_{s-r} and radial tension gradients, during a sunny day

Table 1. Saturated (maximum) axial and radial specific conductivities ($k_{s-a(max)}$ and $k_{s-r(max)}$, respectively) corrected to 20 °C, native embolism estimated as percent loss of conductivity (PLC), tracheid diameter and length and earlywood proportion between outer and inner sapwood at breast height in four 24-year-old Douglas-fir trees. The outer section comprised sapwood rings 1 to 6 and the inner section comprised sapwood rings 7 to 12. Within a row, values with different letters are significantly different at $P < 0.05$.

Radial position	Outer 0.5–2.5 cm	Inner 2.5–4.5 cm
$k_{s-a(max)}$ (kg m^{-1} MPa^{-1} s^{-1})	5.1 ± 0.2 a	3.0 ± 0.5 b
$k_{s-r(max)}$ (10^{-3}, kg m^{-1} MPa^{-1} s^{-1})	1.8 ± 0.4 a	1.3 ± 0.3 a
PLC	17.2 ± 1.4 a	11.0 ± 1.1 b
Tracheid diameter (μm)	31.8 ± 2.6 a	21.7 ± 3.0 b
Tracheid length (mm)	2.7 ± 0.2 a	2.3 ± 0.1 b
Earlywood proportion (%)	67 ± 2 a	69 ± 3 a

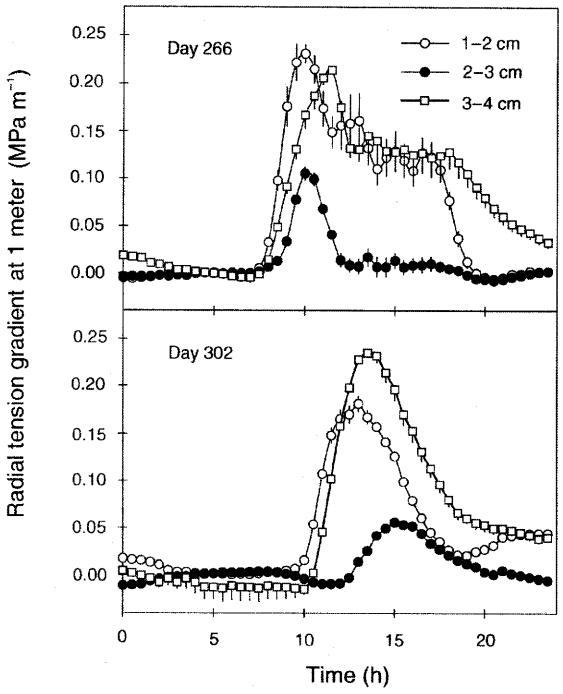

Figure 4. Diurnal courses of radial xylem tension gradients at a stem height of 1 m during a sunny summer day (Day 266) and a cloudy fall day (Day 302). Vertical bars represent standard errors.

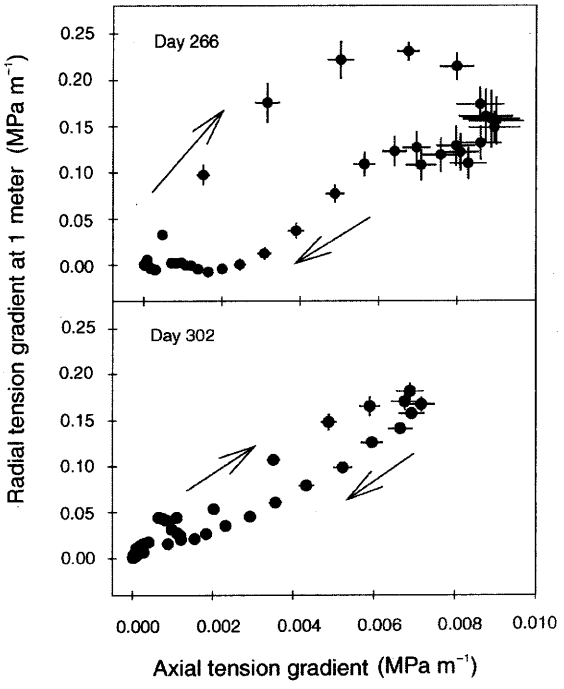

Figure 5. Diurnal course of the radial xylem tension gradient at a stem height of 1 m versus the axial tension gradient in the outer sapwood during a sunny summer day (Day 266) and a cloudy fall day (Day 302). Bars represent standard errors.

the estimated maximum radial J_s at a stem height of 1 m would be 0.38 g m^{-2} s^{-1} in the outer sapwood (rings 1 to 6) and 0.27 g m^{-2} s^{-1} in the inner sapwood (rings 7 to 12) and during an overcast day it would be between 0.25 g m^{-2} s^{-1} in the outer sapwood and 0.14 g m^{-2} s^{-1} in the inner sapwood. At a stem height of 1 m, these radial J_s values are 70–120 times lower than the axial values (Figure 1).

Comparing the diurnal profiles of radial with axial tension gradients revealed a marked hysteresis on a sunny day compared with an overcast day (Figure 5). On a sunny day, the maximum radial tension gradient occurred at 1000 h, which was 120 min earlier than the axial tension gradient maximum. The hysteresis, or departure from the straight line, was 0.003 MPa m^{-1} and 0.001 MPa m^{-1} for a sunny day and a cloudy day, respectively, representing of 35 and 15% of the maximum axial gradients for a sunny day and a cloudy day, respectively.

Earlywood tracheid lumen diameter and tracheid length decreased radially with increasing sapwood depth (Table 1). Measured $k_{s\text{-}a(max)}$ was positively correlated ($P < 0.04$) with both tracheid diameter and length (Figures 6A and 6B). However, compared with variation in tracheid diameter, variation in tracheid length accounted for a substantially greater fraction of variation in $k_{s\text{-}a(max)}$ (76 versus 47%). The theoretical calculated $k_{s\text{-}a}$ was greater ($P < 0.001$) than the measured $k_{s\text{-}a(max)}$ and the difference increased with increasing $k_{s\text{-}a(max)}$ (Figure 7).

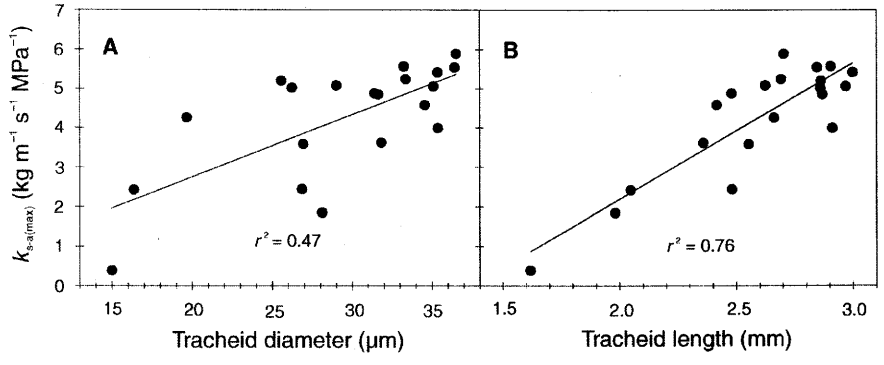

Figure 6. Maximum sapwood axial specific conductivity ($k_{s\text{-}a(max)}$) versus (A) tracheid lumen diameter and (B) tracheid length. Each value represents the mean of two samples taken at each depth in four trees.

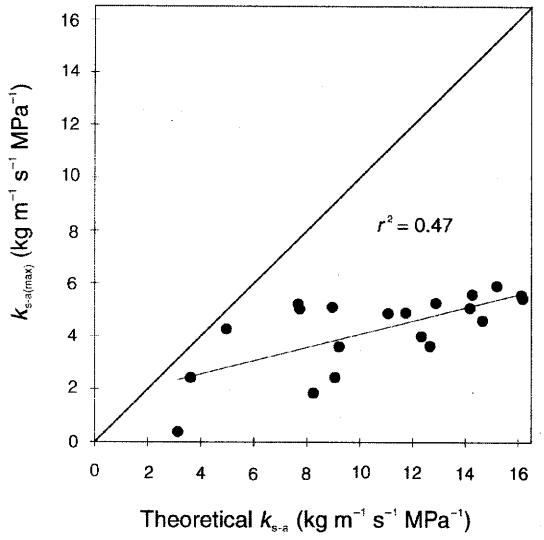

Figure 7. Maximum sapwood axial specific conductivity ($k_{s\text{-}a(max)}$) versus theoretical specific conductivity calculated from Equation 3. The diagonal line represents a 1:1 relationship.

Discussion

Paired measurements of $k_{s\text{-}a}$ and J_s at the same location within Douglas-fir trunks allowed us to estimate the axial and radial tension gradients in situ and to partition sap flow into radial and axial components at the base of the tree. Although J_s on a cool day was only 40% of the maximum on the warmer day, the calculated axial tension gradients were about 75% as great because the higher sap viscosity, due to lower temperature, reduced $k_{s\text{-}a}$. Our results support the hypothesis that large radial tension gradients occur in the sapwood and confirm that transpiration-induced axial tension gradients in trunks are in the range of 0.006–0.01 MPa m^{-1}, not including the gravitational tension gradient.

Calculations of the radial tension gradients were based on the assumption that xylem tension in the outer and inner sapwood was in equilibrium in the morning. Substantial rain events occurred five days before Day 266, which were enough to fully recharge the soil (Warren et al. 2005). Following these rain events and during the whole period studied, the soil water potential and the predawn leaf water potential were in equilibrium, suggesting, first, a complete rehydration of the aboveground part of the trees and, second, that the study trees were not water-stressed. If disequilibrium had occurred (a likely situation during drier periods earlier in the season), an even stronger gradient in radial tension would have existed between inner and outer sapwood. Thus, the estimates presented here are conservative. We would expect absolute xylem tension to be higher in outer sapwood than in inner sapwood because the calculated axial gradients were consistently higher in the outer sapwood (Figure 3).

Scaling up to the full height of the 16-m trees at midday on a sunny day, the total axial transpiration-induced tension difference between the top and the bottom of the unbranched trunk would be 0.1 MPa in the outer sapwood and 0.2 MPa when taking into account the hydrostatic component, whereas the total difference in radial tension between the outer and inner sapwood would be smaller at 0.06 MPa. As shown in small vine shoots (Loviso and Schuber 1998), we can predict that this gradient will increase with stem height because of reductions in diameters and lengths of tracheids with height (Panshin and de Zeeuw 1980), leading to decreasing $k_{s\text{-}a}$ (Domec and Gartner 2001) and increasing J_s (Phillips et al. 2003). Scaling down to the size of a single tracheid using the measured values of tracheid length and width (Table 1), the axial and radial tension gradients at a stem height of 1 m would be around 0.024 and 0.011 kPa per tracheid, respectively. However, near the live crown, at a stem height of 10 m, the radial tension gradient across a single tracheid would be about 0.11 kPa.

When the theoretical hydrostatic gradient of 0.01 MPa m^{-1} is added to our estimates of transpiration-induced tension gradients, total axial gradients would range from 0.016 MPa m^{-1} in the inner sapwood to 0.020 MPa m^{-1} in the outer sapwood. These values agree well with the estimate of ~0.018 MPa m^{-1} obtained for old-growth Douglas-fir trees by the pressure chamber method (Bauerle et al. 1999, Woodruff et al. 2004). In two studies in which axial tension gradients were estimated from measurements of stem $k_{s\text{-}a}$ and published values of J_s, it was concluded that the tension gradients in conifers and hardwoods would be 0.06 and 0.08 MPa m^{-1}, respectively (Heine 1970, 1971). However, these studies may have overestimated the axial water tension gradients by using J_s values measured in the outer sapwood and applying them to the entire sapwood cross section.

When water moves up a tree, sap flux in a given growth ring is largely determined by the rate of transpiration from needles attached to that ring. In this study, the highest axial tension gradient occurred in the outer sapwood, in the samples centered at 1 cm from the cambium (corresponding to the second and third growth rings). This high axial tension is likely caused by transpiration from needles with long-lived leaf connections that are typically sustained for three to five years in Douglas-fir (Balster and Marshall 2000, Weiskittel 2003). We know that foliage can remain alive for many years, but we have little knowledge of how the leaves maintain a connection with the xylem and phloem as the stem expands. Some research suggests that, in conifers, the xylem of the leaf trace breaks as the stem increases in diameter (Elliott 1937, Maton and Gartner 2005). Each year, a cambium at the base of the leaf trace produces new cells that connect the leaf trace to the current year's xylem. Further research on the functionality of needle attachment on the observed J_s would be important for understanding the processes that occur at different depths within the sapwood. For example, the radial patterns of J_s should depend on how long the original xylem connections of the leaf trace remain active.

Inner sapwood had significantly lower $k_{s\text{-}a}$ and $k_{s\text{-}r}$ than outer sapwood. Several studies have shown significant variation in wood $k_{s\text{-}a}$ with radial position in the trunk of conifers, with a

maximum typically occurring in the outermost rings and declining toward the heartwood–sapwood boundary (Booker and Kininmonth 1978, Domec and Gartner 2002, 2003). Trees have a wide range of wood properties that change systematically with distance from the pith (Zobel and van Buijtenen 1989). The low $k_{s\text{-}a}$ in the innermost sapwood can be explained by the smaller tracheid diameter and especially by the smaller tracheid length (Hacke et al. 2004) compared with the outermost sapwood (Figures 6A and 6B). The Hagen–Poiseuille law states that flow rate is proportional to the fourth power of the capillary radius and thus predicts that the large earlywood tracheids are responsible for most of the water flow within a single ring (Zimmerman 1983). This law is frequently used to model xylem transport because it illustrates the importance of small changes in conduit diameter. As found in other studies, measured $k_{s\text{-}a}$ was much less than theoretical $k_{s\text{-}a}$ based on the Hagen–Poiseuille law. Previous attempts to compare measured $k_{s\text{-}a}$ with values predicted from the Hagen–Poiseuille equation indicate that the Hagen–Poiseuille equation significantly overestimates the hydraulic conductivity of xylem conduits (Giordano et al. 1978, Pothier et al. 1989). Rather than being perfect capillaries, Douglas-fir tracheids are typically elliptical in cross section, have spiral-thickened walls and are connected by small diameter pits (5–20 μm) with even smaller membrane pores (0.5–2.0 μm) (Panshin and de Zeeuw 1980). A correction applied to the Hagen–Poiseuille law to account for elliptical conduit cross-section actually increases the discrepancy between measured and theoretical flow rates (Lewis and Boose 1995), indicating an even greater need to identify the cause of these differences.

The difference between inner and outer $k_{s\text{-}r}$ reflected the increase in tracheid length from inner to outer sapwood. A positive correlation exists between tracheid length and pit density and a negative correlation exists between tracheid diameters and pit chamber size (Domec and Gartner, personal observation); shorter tracheids have lower pit densities and bigger pit chambers, which increase the resistance to water transport along the radial pathway (Calkin et al. 1986). In addition, most inter-tracheid pits are on the radial cell walls, facilitating water movement within a growth ring but not between growth rings (Panshin and de Zeeuw 1980). The radial transport of water via tracheids is also reduced by the transition zone from the latewood of one year to the earlywood of the next year, because of reduction in pit density (Bauch et al. 1972). Radial flow may also occur through the cell walls themselves and through ray tracheids, which might play an important role in radial transport of water across several annual rings. The measurements made in this study cannot distinguish between these different pathways.

At a stem height of 1 m, the high radial tension gradients calculated within the inner sapwood and from the inner to the outer sapwood, did not result in high radial J_s because of the low $k_{s\text{-}r}$, which was small compared with $k_{s\text{-}a}$, but similar in magnitude to bulk values of liquid permeability in the transverse direction through green timber (Comstock 1970, Siau 1984). The calculated radial J_s in Douglas-fir sapwood was about 100 times smaller than axial J_s. Although it is difficult to evaluate the significance of this ratio, because no comparable measurements exist for this or other species, it indicates that the use of constant-heat sap flow probes to measure axial J_s is reliable at the base of the trunk because only a minimal correction for radial J_s is necessary. Cooling of the heated probe from radial movement would not cause more than a 1% correction. At a stem height of 10 m, just under the crown, the calculated radial tension gradient would be about 2 MPa m^{-1} and radial J_s would increase to about 10% of axial J_s. However, we can argue that because of a decrease in tracheid lumen and pit size with height (Panshin and DeZeeuw 1980, Domec and Gartner unpublished data), $k_{s\text{-}r}$ would be lower at the top of a tree than at the bottom, which would compensate for the high radial tension gradient and would reduce radial J_s. In addition, it has been shown that to compensate for the decrease in sapwood area with height, J_s is higher at the top of the trunk than at the base (James et al. 2003, Phillips et al. 2003). Therefore, even though the radial tension gradients might increase by a factor of 10 at a stem height of 10 m, the ratio between axial and radial J_s might be lower and correction for radial J_s would still be minimal when using the constant-heat sap flow probes.

Because transpiration "pulls" the sap from the soil to the leaves, water in the xylem is in a metastable state of tension. In this state, the water column is susceptible to embolism, which decreases $k_{s\text{-}a}$ thereby increasing the tension gradient necessary to sustain the same transpiration rate. We found a difference in loss of $k_{s\text{-}a}$ between the outermost and the innermost sapwood rings (Figure 2B, Table 1). The highest rates of native embolism were measured at 1–2 cm from the cambium (Rings 3–7). The oldest sapwood rings (Rings 9–12) and the more recent rings (Rings 1 and 2) had less than half that rate of embolism. Controversial ideas exist for cavitation processes and the ways plants may repair embolism. Direct measurements of radial transport properties may help in understanding the mechanism by which embolized tracheids are refilled because, for a given pressure gradient, the entry of water into a gas-filled tracheid is dictated by its $k_{s\text{-}r}$ (Zwieniecki et al. 2001). We measured higher $k_{s\text{-}r}$ and similar radial tension gradients in the outer sapwood than in the inner sapwood, suggesting facilitated water movement between growth rings in the more recently formed wood. In the outer sapwood, the rate at which water would move through the radial cell wall pits would be more than 40% higher than in the inner sapwood.

Acknowledgments

This research was supported by the USDA Forest Service Ecosystem Processes Program (PNW 02-JV-1126952-252) and the Wind River Canopy Crane Research Facility located within the Wind River Experimental Forest in Washington State, USA. The facility is a cooperative scientific venture among the University of Washington, the USDA Forest Service Pacific Northwest Research Station and Gifford Pinchot National Forest. Sincere thanks to J.M. Warren for help in cutting the trees.

References

Balster, N.J. and J.D. Marshall. 2000. Decreased needle longevity of fertilized Douglas-fir and grand fir in the northern Rockies. Tree Physiol. 20:1191–1197.

Bauch, J., W. Liese and R. Schultze. 1972. The morphological variability of the bordered pit membranes in gymnosperms. Wood Sci. Tech. 6:165–184.

Bauerle, W.L., T.M. Hinckley, J. Èermák, J. Kuèera and K. Bible. 1999. The canopy water relations of old-growth Douglas-fir trees. Trees 13:211–217.

Booker, R.E. and J.A. Kininmonth. 1978. Variation in longitudinal permeability of green radiata wood. N.Z. J. For. Sci. 8:295–308.

Calkin, H.W., A.C. Gibson and P.S. Nobel. 1986. Biophysical model of xylem conductance in tracheids of the fern *Pteris vittata*. J. Exp. Bot. 37:1054–1064.

Clearwater, M.J., F.C. Meinzer, J.L. Andrade, G. Goldstein and N.M. Holbrook. 1999. Potential errors in measurements of nonuniform sap flow using heat dissipation probes. Tree Physiol. 10:367–380.

Cohen, Y., M. Fuchs and G.C. Green. 1981. Improvement of the heat pulse method for determining sap flow in trees. Plant Cell Environ. 4:391–397.

Comstock, G.L. 1970. Directional permeability of softwoods. Wood Fiber 1:283–289.

Dixon, H.H. 1914. Transpiration and the ascent of sap in plants. Macmillan, London, 216 p.

Domec, J.-C. and B.J. Gartner. 2001. Embolism and water storage capacity in bole xylem segments of mature and young Douglas-fir trees. Trees 15:204–214.

Domec, J.-C. and B.J. Gartner. 2002. Age and position-related changes in hydraulic versus mechanical dysfunction of xylem: inferring the design criteria for Douglas-fir wood structure. Tree Physiol. 22:91–104.

Domec, J.-C. and B.J. Gartner. 2003. Relationship between growth rates and xylem hydraulic characteristics in young, mature and old-growth ponderosa pine trees. Plant Cell Environ. 26:471–483.

Donovan, L.A., J.H. Richards and M.J. Linton. 2003. Magnitude and mechanisms of disequilibrium between predawn plant and soil water potentials in desert shrubs. Ecology 84:463–470.

Elliott, J.H. 1937. The development of the vascular system in evergreen leaves more than one year old. Ann. Bot. 1:107–127.

Ford, C.R., M.A. McGuire, R.J. Mitchell and R.O. Teskey. 2004. Assessing variation in the radial profile of sap flux density in *Pinus* species and its effect on daily water use. Tree Physiol. 24: 241–249.

Gartner, B.L. and F.C. Meinzer. 2005. Structure-function relationships in sapwood water transport and storage. *In* Vascular Transport in Plants. Eds. M. Zwieniecki and N.M. Holbrook. Elsevier, Oxford, pp 307–331.

Giordano, R., A. Salleo, S. Salleo and F. Wanderlingh. 1978. Flow in xylem vessels and Poiseuille's law. Can. J. Bot. 56:333–338.

Granier, A. 1985. Une nouvelle méthode pour la mesure du flux de sève brute dans le tronc des arbres. Ann. Sci. For. 42:193–200.

Hacke, U.G., J.S. Sperry and J. Pittermann. 2004. Analysis of circular bordered pit function II. Gymnosperm tracheids with torus-margo pit membranes. Am. J. Bot. 91:386–400.

Heine, R.W. 1970. Estimation of conductivity and conducting area of poplar stems using a radioactive tracer. Ann. Bot. 34:1019–1024.

Heine, R.W. 1971. Hydraulic conductivity in trees. J. Exp. Bot. 72: 503–511.

Hellkvist, J., G.P. Richards and P.G Jarvis. 1974. Vertical gradients of water potential and tissue water relations in Sitka spruce trees measured with the pressure chamber. J. App. Ecol. 11:637–667.

Herrington, L.P. 1969. On temperature and heat flow in tree stems. School of Forestry Bulletin 73, Yale University, 79 p.

James, S., M.J. Clearwater, F.C. Meinzer and G. Goldstein. 2002. Heat dissipation sensors of variable length for the measurement of sap flow in trees with deep sapwood. Tree Physiol. 22: 277–283.

James, S., F.C. Meinzer, G. Goldstein, D. Woodruff, T. Jones, T. Restom, M. Mejia, M. Clearwater and P. Campanello. 2003. Axial and radial water transport and internal water storage in tropical forest canopy trees. Oecologia 134:37–45.

Lewis, A.M. and E.R. Boose. 1995. Estimating volume flow rates through xylem conduits. Am. J. Bot. 82:1112–1116.

Loviso, C. and A. Schuber 1998. Effects of water stress on vessel size and xylem hydraulic conductivity in *Vitis vinifera* L. J. Exp. Bot. 49:693–700.

Mark, W.R. and D.L. Crews. 1973. Heat-pulse velocity and bordered pit condition in living Engelmann spruce and Lodgepole pine trees. For. Sci. 19:291–296.

Maton, C. and B.L. Gartner. 2005. Gymnosperm needles pull water through the xylem produced in the same year as the needle? Am. J. Bot. 92:123–130.

Monteith, J.L. and M.H. Unsworth. 1990. Principles of environmental physics. 2nd Edn. Edwards Arnold, London, 291 p.

Nadezhdina, N., J. Èermák and R. Ceulemans. 2002. Radial patterns of sap flow in woody stems of dominant and understory species: scaling errors associated with positioning of sensors. Tree Physiol. 22:907–918.

Panshin, A.J. and C. de Zeeuw. 1980. Textbook of wood technology. McGraw-Hill, 722 p.

Phillips, N., R. Oren and R. Zimmermann. 1996. Radial patterns of xylem sap flow in non diffuse- and ring- porous tree species. Plant Cell Environ. 19:983–990.

Phillips, N., M.G. Ryan, B.J. Bond, N.G. McDowell, T.M. Hinckley and J. Èermák. 2003. Reliance on stored water increases with tree size in three species in the Pacific Northwest. Tree Physiol. 23: 237–245.

Pothier, D., H.A. Margolis, J. Poliquin and R.H. Waring. 1989. Relation between the permeability and the anatomy of jack pine sapwood with stand development. Can. J. For. Res. 19:1564–1570.

Rasband, W. 1996. NIH Image. National Institutes of Health, Bethesda, MD.

Scholander, P.F., H.T. Hammel, E.D. Bradstreet and E.A. Hemmingsen. 1965. Sap pressure in vascular plants. Science 148:339–346.

Siau, J.F. 1984. Transport processes in wood. Springer-Verlag, New York, 245 p.

Spearing, W.E. and I.H. Isenberg. 1947. The maceration of woody tissue with acetic acid and sodium chlorite. Science 105:214.

Spicer, R. and B.L. Gartner. 1998. How does a gymnosperm branch assume the hydraulic status of a main stem when it takes over a leader? Plant Cell Environ. 21:1063–1070.

Spicer, R. and B.L. Gartner. 2001. The effects of cambial age and position within the stem on specific conductivity in Douglas-fir sapwood. Trees 15:222–229.

Tison, A. 1903. Les traces foliaires des conifères dans leur rapport avec l'épaississement de la tige. Mém. Soc. Linn. Normandie 21: 61–81.

Tyree, M.T. 1988. A dynamic model for water flow in a single tree. Tree Physiol. 4:195–217.

Tyree, M.T., D.A. Snyderman, T. Wilmot and J.L. Machado. 1991. Water relations and hydraulic architecture of a tropical tree (*Schefflera morotoni*). Plant Physiol. 96:1105–1113.

Tyree, M.T., B. Sinclair, P. Lu and A. Granier. 1993. Whole shoot hydraulic resistance in *Quercus* species measured with a new high-pressure flowmeter. Ann. Sci. For. 50:417–423.

Warren, J.M., F.C. Meinzer, J.R. Brooks and J.-C. Domec. 2005. Vertical stratification of soil water storage and release dynamics in Pacific Northwest coniferous forests. Agric. For. Meteorol. 130: 39–58.

Weiskittel, A.R. 2003. Alterations in Douglas-fir crown structure, morphology and dynamics imposed by the Swiss needle cast disease in the Oregon Coast Range. M.Sc. Thesis, Dept. of Forest Resources, Oregon State University, 389 p.

Woodruff, D., B.J. Bond and F.C. Meinzer. 2004. Does leaf turgor limit tree height? Plant Cell Environ. 27:229–236.

Yang, S.D. and M.T. Tyree. 1994. Hydraulic architecture of *Acer saccharum* and *A. rubrum*: comparison of branches to whole trees and the contribution of leaves to hydraulic resistance. J. Exp. Bot. 45:179–186.

Zimmerman, M.H. 1983. Xylem structure and the ascent of Sap. Springer-Verlag, Berlin-Heidelberg-New York, 143 p.

Zobel, B.H. and J.P. van Buijtenen. 1989. Variation among and within trees. *In* Wood Variation: Its Causes And Control. Springer-Verlag, New York, pp 189–217.

Zwieniecki, M., P.J. Melcher and N.M. Holbrook. 2001. Hydraulic properties of individual xylem vessels of *Fraxinus americana*. J. Exp. Bot. 52:257–264.